

Spontaneous autophoretic motion of isotropic particles

Sébastien Michelin,^{1, a)} Eric Lauga,² and Denis Bartolo³

¹⁾*LadHyX – Département de Mécanique, Ecole polytechnique, 91128 Palaiseau Cedex, France*

²⁾*Department of Mechanical and Aerospace Engineering, University of California San Diego, 9500 Gilman Drive, La Jolla CA 92093, USA.*

³⁾*Laboratoire de Physique, Ecole Normale Supérieure de Lyon, Université de Lyon and CNRS, 46, allée d'Italie, F-69007 Lyon, France*

(Dated: 28 June 2018)

Suspended colloidal particles interacting chemically with a solute can self-propel by autophoretic motion when they are asymmetrically patterned (Janus colloids). Here we demonstrate theoretically that such anisotropy is not necessary for locomotion and that the nonlinear interplay between surface osmotic flows and solute advection can produce spontaneous, and self-sustained motion of isotropic particles. Solving the classical autophoretic framework for isotropic particles, we show that, for given material properties, there exists a critical particle size (or Péclet number) above which spontaneous symmetry-breaking and autophoretic motion occur. A hierarchy of instabilities is further identified for quantized critical Péclet numbers.

The locomotion of microorganisms has long been used as a motivation and a practical inspiration for the design of synthetic self-propelled particles. Typically, biological cells generate propulsion by deforming their slender appendages, termed flagella or cilia, in a non-time-reversible fashion¹. However, and perhaps not surprisingly given the numerous microfabrication challenges, no genuinely self-propelled micro-swimmer has been manufactured in the lab so far. Instead, man-made biomimetic propellers are driven by external torques or forces. That actuation allows either to deform soft propellers whose deformed shape induce propulsion^{2–4}, to continuously generate propulsion in chiral shapes^{5,6}, or to exploit interactions with surfaces^{7–9}.

An alternative route for the production of artificial small-scale swimmers has proven to be much more successful. It consists in making miniaturized chemically powered “engines” with no moving parts, typically made of reactive Janus beads or rods^{10–12}. The reaction products released by these chemically-asymmetric particles create concentration gradients which induce a net phoretic fluid motion near their surface leading to locomotion. Theoretically, the interest in these so-called autophoretic swimmers was triggered by a theoretical model which accounted for such a novel propulsion mechanism in a simple and generic fashion^{13,14}. This model was then further elaborated to include the nonlinear interplay between the colloid motion and the advection of the reactants^{15–17} or a more complex kinetic route for the surface chemistry¹⁸, to deal with the rotational Brownian motion of the swimmers¹⁹, and to detail the microscopic coupling between the concentration gradients and the fluid flows at small scales²⁰.

In order to self-propel, autophoretic swimmers are chemically patterned, and it is the asymmetries in the chemical reactions on their surfaces which are responsible for locomotion in the first place. This requirement would make it thus difficult to achieve high-throughput production. An ingenious solution to such an engineering issue was recently offered with the production of isotropic self-propelled Marangoni droplets²¹. In a mechanism akin to the one responsible for the spontaneous motion of reactive droplets surfing on fluid interfaces^{22,23}, a net flow is induced around the droplets by interfacial stresses arising from the self-generated gradients of reactive surfactants^{21,24,25}. Unlike autophoretic Janus particles which swim as a result of built-in design asymmetries, the concentration of surfactant molecules at the surface of reactive droplets is spontaneously broken, leading to propulsion.

In this Letter, we demonstrate that asymmetry in the shape or the chemistry of the colloidal particle, assumed in most existing studies on autophoretic swimmers^{13–16,18}, is not necessary for locomotion. We show that isotropic spherical particles can achieve self-propulsion through a spontaneous symmetry-breaking mechanism, a route to locomotion akin to that of a larger variety of biological systems²⁶. We solve analytically the classical nonlinear autophoretic theoretical framework at arbitrary Péclet number. We show that, for a given set of material properties, there exists a critical particle size above which the non-swimming purely diffusive state is unstable and spontaneous autophoretic motion occurs. In addition, the flow induced by the reactive particles displays a hierarchy of instabilities associated with quantized critical Péclet numbers. Using numerical solutions of the full unsteady diffusiophoretic problem we confirm our analytical

^{a)}Electronic mail: sebastien.michelin@ladhyx.polytechnique.fr

predictions and show that, above the instability threshold, isolated isotropic particles reach, after a transient, a steady swimming state with broken front-back symmetry in the concentration field and the hydrodynamic signature of a “pusher” swimmer.

We consider a spherical particle of radius a located in a Newtonian fluid of shear viscosity η . We focus on the limit of steady Stokes flow so that the inertia of both the fluid and the particle is negligible. The sphere is chemically active and either emits or captures a single type of solute particles with an isotropic surface emission rate denoted $\mathcal{A}^{13,14}$. Within the standard minimal framework, we ignore in what follows the specifics of the chemical reaction occurring at its surface, and all other reactants and reaction products, which are assumed to interact only weakly with the particle. The solute interacts with the spherical particle through a short-range potential and we focus on the classical limit $\lambda \ll a$, with λ the characteristic potential range²⁷.

Tangential gradients in solute concentration induce a net slip (phoretic) velocity outside the diffuse layer, together with a tangential (Marangoni) stress discontinuity at the particle surface^{17,27}. For a solid particle, Marangoni stresses vanish, and the phoretic slip velocity is set by the local chemical-potential gradient parallel to the surface²⁸. For small variations of the concentration, $c(\mathbf{r}, t)$, its azimuthal component is given by

$$u_\theta(r = a) = \frac{\mathcal{M}}{a} \frac{\partial c}{\partial \theta}. \quad (1)$$

The mobility, $\mathcal{M} \sim \pm k_B T \lambda^2 / \eta$, can either be positive or negative depending on the form of the solute-surface interactions (k_B is the Boltzmann constant, and T the temperature)²⁷. Assuming that the solute has a molecular diffusivity \mathcal{D} , the typical autophoretic velocity which sets the swimming speed of a Janus colloid is $\mathcal{V} = |\mathcal{A}\mathcal{M}|/\mathcal{D}^{14}$. Non-dimensionalizing velocities, lengths, and concentrations in the transport equations by \mathcal{V} , a , and $a|\mathcal{A}|/\mathcal{D}$ respectively, the coupled fluid flow- solute advection-diffusion problem takes the form

$$\nabla^2 \mathbf{u} = \nabla p, \quad \nabla \cdot \mathbf{u} = 0, \quad (2)$$

$$|\text{Pe}| \left(\frac{\partial c}{\partial t} + \mathbf{u} \cdot \nabla c \right) = \nabla^2 c, \quad (3)$$

where we have defined the (signed) Péclet number as $\text{Pe} = \mathcal{A}\mathcal{M}a/\mathcal{D}^2$. We henceforth consider axisymmetric solutions only, so that in spherical polar coordinates the solute concentration is written as $c(r, \mu, t)$ with $\mu \equiv \cos \theta$, and only rectilinear motion along the axis of symmetry \mathbf{e}_z is considered. In dimensionless units, the surface activity and the particle mobility become unitary numbers, $A = \mathcal{A}/|\mathcal{A}| = \pm 1$, $M = \mathcal{M}/|\mathcal{M}| = \pm 1$, and the boundary conditions in the far-field and on the particle surface become

$$\mathbf{u}(r \rightarrow \infty) = -U\mathbf{e}_z, \quad c(r \rightarrow \infty) = c_\infty, \quad (4)$$

$$\frac{\partial c}{\partial r}(r = 1) = -A, \quad u_r(r = 1) = 0, \quad (5)$$

$$u_\theta(r = 1) = -M\sqrt{1 - \mu^2} \frac{\partial c}{\partial \mu}(r = 1). \quad (6)$$

In Eq. (4), $U(t)$ is the dimensionless swimming velocity, obtained from the force-free condition. Using the reciprocal theorem, $U(t)$ is found to be the surface average of the slip velocity^{14,29} and, using Eq. (1), is written in terms of the first moment of $c(1, \mu, t)$ as

$$U(t) = -M \int_{-1}^1 \mu c(1, \mu, t) d\mu. \quad (7)$$

The dimensionless problem is then fully characterized by the signs of both A and M , the far-field concentration, c_∞ , and the value of $|\text{Pe}|$.

In the case of uniform surface activity (constant value of A), a trivial solution exists at all Pe numbers, namely the solute concentration is isotropic, $\bar{c} = A/r + c_\infty$, leading to no net flow ($\bar{\mathbf{u}} = 0$) and zero swimming velocity ($\bar{U} = 0$). However, both the solute transport equation, Eq. (3), and the boundary conditions on the particle, Eq. (6), couple the swimming problem with the solute dynamics. A small fluctuation of the particle velocity would result in a polar perturbation of the flow field. Due to the nonlinear convective coupling, $\mathbf{u} \cdot \nabla c$, this velocity fluctuation would lead to a polarization of the concentration field around the

finite-size particle. In turn, the first moment of the surface concentration, $c(1, \mu, t)$, would become finite and, depending on its sign in relation to the initial perturbation, increase or decrease the particle velocity through Eq. (7). If the velocity decreased, the initial perturbation would be stabilized, and no net motion could occur as a result of an infinitesimal fluctuation. However, if the velocity increased, the broken symmetry in the solute concentration would be amplified, and spontaneous motion would occur.

To quantify the conditions for spontaneous motion, we analytically investigate the stability of the isotropic state. Defining $c = \bar{c} + c'$, $\mathbf{u} = \mathbf{u}'$, $U = U'$, and subsequently dropping the primes to denote perturbations, the Stokes flow problem around the sphere can be solved analytically using the so-called squirring modes decomposition^{30,31}. The streamfunction ψ and solute concentration c are decomposed azimuthally onto orthogonal modes

$$\psi(r, \mu, t) = \sum_{n=1}^{\infty} \frac{2n+1}{n(n+1)} \alpha_n(t) \psi_n(r) (1-\mu^2) L'_n(\mu), \quad c(r, \mu, t) = \sum_{n=0}^{\infty} c_n(r, t) L_n(\mu), \quad (8)$$

with $\psi_1(r) = (1-r^3)/3r$, $\psi_n(r) = (r^{-n} - r^{-n+2})/2$ for $n \geq 2$, and $L_n(\mu)$ the n -th Legendre polynomial. The squirring mode intensities, $\alpha_n(t)$, are obtained directly from the slip velocity on the particle surface³¹, as

$$\alpha_n(t) = \frac{1}{2} \int_{-1}^1 \sqrt{1-\mu^2} L'_n(\mu) u_\theta(r=1, \mu, t) d\mu. \quad (9)$$

The first mode is the only one contributing to the swimming velocity ($\alpha_1(t) = U(t)$), and is therefore termed the swimming mode. The second mode corresponds to the flow created by a stresslet (i.e. a force dipole)³². Higher order modes correspond to higher order singularities decaying faster in the far field.

Because the trivial solution is isotropic, we can project both the advection-diffusion equation, Eq. (3), and the definition of the slip velocity, Eq. (6), along these modes, and obtain a set of independent problems for $\{\alpha_n(t), c_n(r, t)\}$. For $n = 1$, this leads to the following inhomogeneous eigenvalue problem for the first moment of the concentration profile, $c_1(r, t)$:

$$|\text{Pe}| \frac{\partial c_1}{\partial t} - \frac{1}{r^2} \left[\frac{\partial}{\partial r} \left(r^2 \frac{\partial c_1}{\partial r} \right) - 2c_1 \right] = \frac{U \text{Pe}}{Mr^2} \left(\frac{1}{r^3} - 1 \right), \quad (10)$$

$$U(t) = -\frac{2}{3} M c_1(1, t), \quad c'_1(1, t) = 0, \quad c_1(r \rightarrow \infty, t) \sim 0. \quad (11)$$

Note that the first moment, c_1 , evaluated at $r = 1$ is proportional to the instantaneous swimming speed of the particle, (Eq. 11). Looking for eigenmodes of the form $c_1(r, t) = e^{\sigma t} c(r)$, it can be shown that all eigenvalues σ of Eqs. (10)–(11) are real, and that any $\sigma < 0$ is a solution. We focus here exclusively on potential unstable modes ($\sigma > 0$) and define $\beta \equiv \sqrt{\sigma |\text{Pe}|} > 0$. Introducing the rescaled radial variable $x \equiv \beta r$, the function $C(x) \equiv c(\beta x)$ satisfies

$$\frac{d}{dx} \left(x^2 \frac{dC}{dx} \right) - (2 + x^2) C = \frac{2\text{Pe}}{3} \left(\frac{\beta^3}{x^3} - 1 \right). \quad (12)$$

The general solution of Eq. (12) satisfying the far-field condition $C(x \rightarrow \infty) = 0$ is

$$C(x) = \frac{2\text{Pe}}{3} \left\{ \frac{1}{x^2} + \beta^3 \left[\frac{A(x)}{8x^2} + \frac{B(x)}{8x} + \frac{1}{4x^3} \right] \right\} + \frac{be^{-x}(1+x)}{x^2} \quad (13)$$

where b is an integration constant to be determined, and $A(x) = \sinh(x)\text{Chi}(x) - \cosh(x)\text{Shi}(x)$, and $B(x) = \sinh(x)\text{Shi}(x) - \cosh(x)\text{Chi}(x)$, with $\text{Chi}(x)$ and $\text{Shi}(x)$ being the hyperbolic cosine and sine integral functions respectively³³. Applying the two boundary conditions on the sphere, $C'(1) = 0$, and $C(1) = 1$, and using the definitions of $A(x)$ and $B(x)$ yields a final implicit expression for the growth rate, $\sigma = \beta^2/|\text{Pe}|$, as a function of the signed Péclet number

$$\text{Pe} = \frac{12\beta^2 + 24\beta + 24}{\beta^4 \int_{\beta}^{\infty} \frac{e^{\beta-t}}{t} dt + 6 + \beta^2 - \beta^3 - 2\beta}. \quad (14)$$

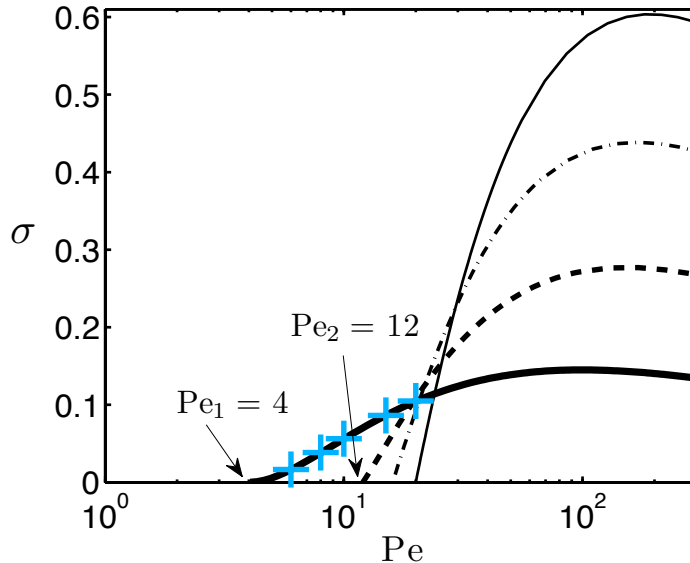


FIG. 1. (Color online) Growth rate of the unstable swimming mode (theoretical prediction, solid line) as a function of the Péclet number, Pe , for emitting particles and positive mobility ($A = M = 1$). Spontaneous symmetry-breaking of the concentration field and swimming occur at $Pe = 4$. The crosses represent the growth rate of the swimming mode $n = 1$ as obtained from numerical simulations of the full unsteady problem. The growth rate of the unstable modes of azimuthal order $n = 2, 3$ and 4 are also shown (theoretical prediction, dashed, dash-dotted and thin-solid, respectively). Note that the hierarchy in the growth rates is reversed at high Pe .

For positive values of β , the right-hand side of Eq. (14) is strictly greater than 4. For any value of Pe above this critical value, a single positive value of β exists such that Eq. (14) is satisfied. Consequently, the fluctuations of the first moment, c_1 , and the particle swimming speed, U , are exponentially amplified if the condition $Pe \geq Pe_1 = 4$ is satisfied. Given that Pe is a signed quantity, the instability condition requires that $MA = 1$. Particles with positive (resp. negative) mobility M are unstable only if they have a positive (resp. negative) flux \mathcal{A} corresponding to the case of emitting (resp. absorbing) the solute on the particle surface. The growth rate of the unstable swimming mode is shown as a function of Pe in Fig. 1 (solid line). The existence of a critical Péclet number implies that there exists a critical particle radius above which an isotropic reactive particle would undergo spontaneous motion. Recently, a study of light-activated colloids reported the spontaneous surfing motion of reactive isotropic colloids lying on a solid surface³⁴, a system which might be a potential candidate to test, at least qualitatively, our predictions.

In order to further investigate the possibility for long-time self-propulsion, we need to go beyond the above linear stability analysis and check whether the asymptotic state of the concentration field is compatible with swimming. In order to do so, numerical simulations of the full unsteady diffusiophoretic problem, Eqs. (2)–(6), are performed: the Stokes flow problem is solved explicitly using the squirmer mode decomposition, and the advection-diffusion problem is marched in time using a semi-explicit scheme, finite differences in the radial directions, and the Legendre spectral decomposition for the azimuthal dependence³⁵. A small velocity perturbation is imposed on the spherical particle initially at rest. Regardless of the amplitude of the initial perturbation, the system is stable and returns to its initial rest state after perturbation for $Pe < 4$. In contrast, when $Pe > 4$, the swimming velocity of the particle grows exponentially, and the growth rates obtained numerically are in quantitative agreement with our analytic predictions, see Fig. 1.

Turning to the long-time behavior, our computations confirm that the asymptotic state of the concentration field is compatible with locomotion. This is illustrated in Fig. 2 for $Pe = 6$, where we plot the time-evolution of the instantaneous particle swimming speed (thick solid line). Three typical snapshots in Fig. 2 (see also the associated video) illustrate the corresponding evolution of the solute concentration field. A steady state is reached and the swimming speed plateaus to a finite value in the long-time limit (note the surprising existence of a local maximum velocity during the transient dynamics). Repeating the simulations for a range of Péclet numbers, we plot in Fig. 3 the nonlinear variation of the long-time swimming velocity, U^∞ , as a function of Pe . Figure 3 demonstrates the supercritical nature of the autophoretic instability: for

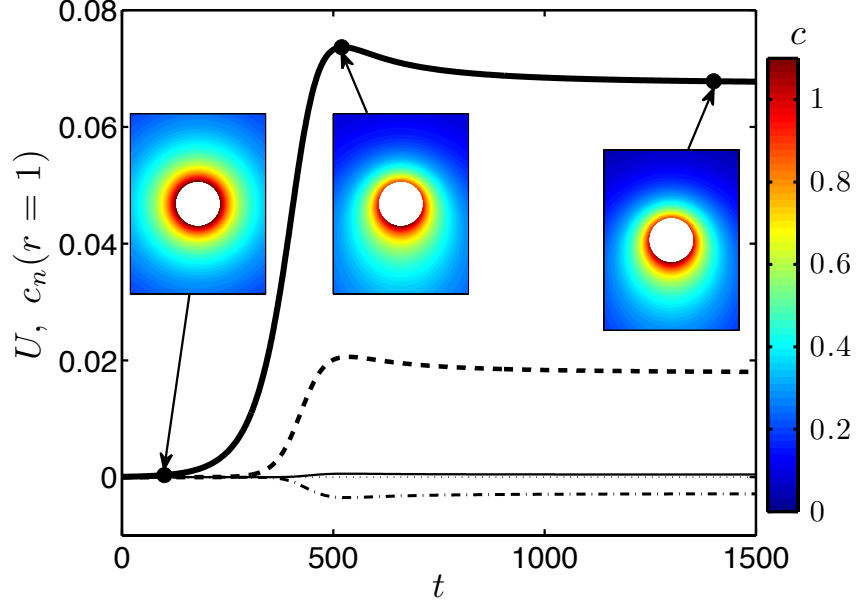


FIG. 2. (Color online) Time-evolution of the instantaneous swimming velocity, $U(t)$ (thick solid line), and of three higher squirring modes, $c_n(r = 1, t)$: mode $n = 2$, which corresponds to the magnitude of the stresslet (dashed line), $n = 3$ (dash-dotted line) and $n = 4$ (thin solid line). Results are displayed for $Pe = 6$ and $AM = 1$. The solute concentration is shown at three different times revealing the establishment of a front-back asymmetry for an upward swimming motion (see Supplementary video)

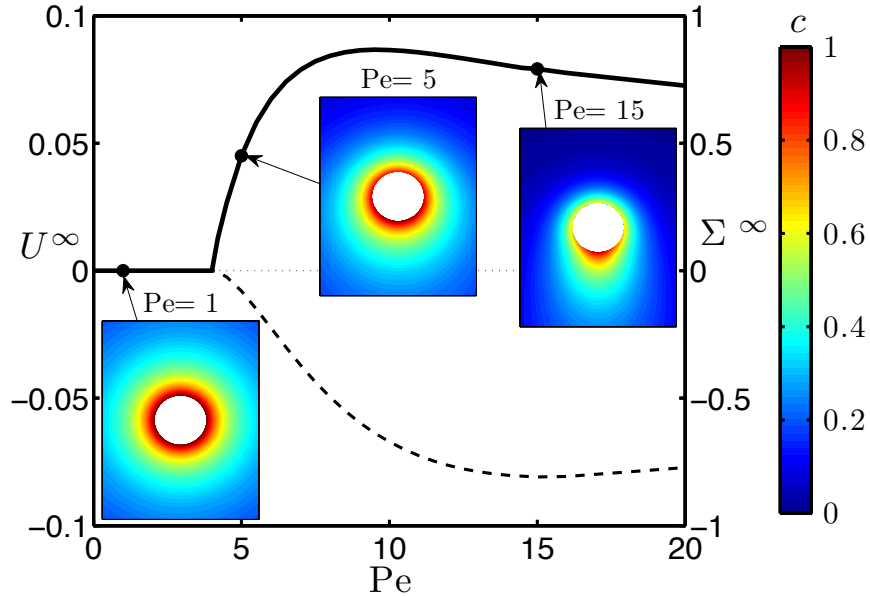


FIG. 3. (Color online) Long-time spontaneous swimming velocity, U^∞ (solid line), and magnitude of the long-time induced stresslet, $\Sigma^\infty \equiv -4\pi M c_2(r = 1, t = \infty)$ (dashed line), as a function of the Péclet number (with $AM = 1$). The steady state solute distribution around the particle is shown for $Pe = 1$, $Pe = 5$, and $Pe = 15$ for an upward swimming motion. The swimmer is always a “pusher” in the far field.

$Pe > 4$, any infinitesimal perturbation of the isotropic state will lead to spontaneous self-propulsion. Note the non-monotonic variation with an optimal value of $Pe \approx 9$ leading to the highest asymptotic swimming speed.

So far we focused exclusively on unstable swimming modes. In order to address the collective dynamics of such particles, it is necessary to consider higher order squirmer modes. Repeating, for $n \geq 2$, the theoretical approach presented above for $n = 1$, we can obtain the unstable growth rates of each mode as a function of Pe . The results reveal a hierarchy of supercritical instabilities corresponding to an infinite set of quantized critical Péclet numbers, $Pe_n = 4(n + 1)$, for mode n . This hierarchy of instabilities is illustrated in Fig. 1 where we plot the dependence of the growth rates for modes 2, 3, and 4 on the Péclet number. Notably, the stresslet mode becomes unstable at $Pe_2 = 12$.

Beyond linear analysis, the saturation of the swimming velocity results from the nonlinear evolution of concentration fluctuations having a $n = 1$ symmetry into higher-order n -modes, as shown in Fig. 2. Although the Péclet number is below the critical value for all modes but the first one to be unstable ($Pe = 6$ in Fig. 2), the nonlinear dynamics leads non-zero values for the other modes (modes 2, 3, and 4 are shown in Fig. 2). In particular, the long-time value of the induced stresslet, Σ^∞ , is shown in Fig. 3. Independently of the signs of both \mathcal{A} and \mathcal{M} , the unstable particle induces in the far field a flow with the symmetry of a “pusher” swimmer, similarly to flagellated bacteria¹.

Similarly to Marangoni flows which have been observed for over 100 years to trigger the self-propulsion of camphor boats floating on water, we demonstrated in this letter that self-phoretic flows past isotropic particles show an instability to a spontaneous swimming state. The phenomenon discovered here could be exploited to readily design self-propelled “submarines” out of isotropic colloidal particles. Although our description of the surface chemistry is particularly simple (a fixed-rate absorption or release of solute), the instability and self-propulsion mechanism remain in fact valid for a much broader class of surface chemistry (see supplementary material³⁶). These results are expected to be applicable generically to particles of different shapes or interacting with many chemical species, and suggest a simple experimental model system to carry out physical studies of active systems.

We acknowledge valuable discussions with Olivier Dauchot and John Brady. This work was supported in part by the NSF through grant number CBET-0746285 (EL).

- ¹E. Lauga and T. Powers, “The hydrodynamics of swimming microorganisms,” *Rep. Prog. Phys.* **72**, 096601 (2009).
- ²R. Dreyfus, J. Baudry, M. L. Roper, M. Fermigier, H. A. Stone, and J. Bibette, “Microscopic artificial swimmers,” *Nature* **437**, 862 (2005).
- ³W. Gao, S. Sattayasamitsathit, K. M. Manesh, D. Weihs, and J. Wang, “Magnetically powered flexible metal nanowire motors,” *J. Am. Chem. Soc.* **132**, 14403 (2010).
- ⁴O. S. Pak, W. Gao, J. Wang, and E. Lauga, “High-speed propulsion of flexible nanowire motors: Theory and experiments,” *Soft Matter* **7**, 8169 (2011).
- ⁵A. Ghosh and P. Fischer, “Controlled propulsion of artificial magnetic nanostructured propellers,” *Nano Lett.* **9**, 2243 (2009).
- ⁶S. Tottori, L. Zhang, F. Qiu, K. K. Krawczyk, A. Franco-Obregon, and B. J. Nelson, “Magnetic helical micromachines: Fabrication, controlled swimming, and cargo transport,” *Adv. Mat.* **24**, 811816 (2012).
- ⁷P. Tierno, O. Guell, F. Sagues, R. Golestanian, and I. Pagonabarraga, “Controlled propulsion in viscous fluids of magnetically actuated colloidal doublets,” *Phys. Rev. E* **81**, 011402 (2010).
- ⁸C. E. Sing, L. Schmid, M. F. Schneider, T. Franke, and A. Alexander-Katz, “Controlled surface-induced flows from the motion of self-assembled colloidal walkers,” *Proc. Natl. Acad. Sci. USA* **107**, 535 (2010).
- ⁹L. Zhang, T. Petit, Y. Lu, B. E. Kratochvil, K. E. Peyer, J. L. Ryan Pei, and B. J. Nelson, “Controlled propulsion and cargo transport of rotating nickel nanowires near a patterned solid surface,” *ACS Nano* **4**, 6228 (2010).
- ¹⁰J. R. Howse, R. A. L. Jones, A. J. Ryan, T. Gough, R. Vafabakhsh, and R. Golestanian, “Self-Motile Colloidal Particles: From Directed Propulsion to Random Walk,” *Phys. Rev. Lett.* **99**, 048102 (2007).
- ¹¹S. J. Ebbens and J. R. Howse, “In pursuit of propulsion at the nanoscale,” *Soft Matter* **6**, 726 (2010).
- ¹²G. Zhao and M. Pumera, “Macroscopic Self-Propelled Objects,” *Chem. Asian J.* **7**, 1994 (2012).
- ¹³R. Golestanian, T. B. Liverpool, and A. Ajdari, “Propulsion of a molecular machine by asymmetric distribution of reaction products,” *Phys. Rev. Lett.* **94**, 220801 (2005).
- ¹⁴R. Golestanian, T. B. Liverpool, and A. Ajdari, “Designing phoretic micro- and nano-swimmers,” *New J. Phys.* **9**, 126 (2007).
- ¹⁵U. M. Córdova-Figueroa and J. F. Brady, “Osmotic Propulsion: The Osmotic Motor,” *Phys. Rev. Lett.* **100**, 158303 (2008), see also the comments and replies associated with this article.
- ¹⁶J. F. Brady, “Particle motion driven by solute gradients with application to autonomous motion: continuum and colloidal perspectives,” *J. Fluid Mech.* **667**, 216 (2011).
- ¹⁷F. Jülicher and J. Prost, “Generic theory of colloidal transport,” *Eur. Phys. J. E* **29**, 27 (2009).
- ¹⁸S. Ebbens, M.-H. Tu, J. R. Howse, and R. Golestanian, “Size dependence of the propulsion velocity for catalytic janus-sphere swimmers,” *Phys. Rev. E* **85**, 020401 (2012).
- ¹⁹R. Golestanian, “Anomalous Diffusion of Symmetric and Asymmetric Active Colloids,” *Phys. Rev. Lett.* **102**, 188305 (2009).
- ²⁰B. Sabass and U. Seifert, “Nonlinear, electrocatalytic swimming in the presence of salt,” *J. Chem. Phys.* **136**, 214507 (2012).
- ²¹S. Thutupalli, R. Seemann, and S. Herminghaus, “Swarming behavior of simple model squirmers,” *New J. Phys.* **13**, 073021 (2011).

- ²²Y. Sumino, N. Magome, T. Hamada, and K. Yoshikawa, "Self-Running Droplet: Emergence of Regular Motion from Nonequilibrium Noise," *Phys. Rev. Lett.* **94**, 068301 (2005).
- ²³T. Toyota, N. Maru, M. M. Hanczyc, T. Ikegami, and T. Sugawara, "Self-Propelled Oil Droplets Consuming "Fuel" Surfactant," *J. Am. Chem. Soc.* **131**, 5012 (2009).
- ²⁴N. Yoshinaga, K. H. Nagai, Y. Sumino, and H. Kitahata, "Drift instability in the motion of a fluid droplet with a chemically reactive surface driven by marangoni flow," *Phys. Rev. E* **86**, 016108 (2012).
- ²⁵A. K. Schmid, N. C. Bartelt, and R. Q. Hwang, "Alloying at Surfaces by the Migration of Reactive Two-Dimensional Islands," *Science* **290**, 1561 (2000).
- ²⁶J. van der Gucht and C. Sykes, "Physical model of cellular symmetry breaking," *Cold Spring Harb. Perspect. Biol.* **1**, a001909 (2009).
- ²⁷J. L. Anderson, "Colloid transport by interfacial forces," *Ann. Rev. Fluid Mech.* **21**, 61 (1989).
- ²⁸D. C. Prieve and R. Roman, "Diffusiophoresis of a rigid sphere through a viscous electrolyte solution," *J. Chem. Soc. Far. Trans.* **83**, 1287 (1987).
- ²⁹H. A. Stone and A. D. T. Samuel, "Propulsion of microorganisms by surface distortions," *Phys. Rev. Lett.* **77**, 4102 (1996).
- ³⁰J. R. Blake, "A spherical envelope approach to ciliary propulsion," *J. Fluid Mech.* **46**, 199 (1971).
- ³¹S. Michelin and E. Lauga, "Optimal feeding is optimal swimming for all Péclet numbers," *Phys. Fluids* **23**, 101901 (2011).
- ³²G. K. Batchelor, "The stress system in a suspension of force-free particles," *J. Fluid Mech.* **41**, 545 (1970).
- ³³M. Abramowitz and I. A. Stegun, *Handbook of Mathematical Functions with Formulas, Graphs, and Mathematical Tables* (Dover, New York, 1964).
- ³⁴J. Palacci, S. Sacanna, A. P. Steinberg, D. J. Pine, and P. M. Chaikin, "Living crystals of light-activated colloidal surfers," *Science* **22**, 936 (2013).
- ³⁵S. Michelin and E. Lauga, "Unsteady feeding and optimal strokes of model ciliates," *J. Fluid Mech.* **715**, 1 (2013).
- ³⁶See supplementary material that demonstrates that the spontaneous motion is a generic mechanism which applies to more realistic reaction kinetics.